

THE TALENTED MR. INVERSIVE TRIANGLE IN THE ELLIPTIC BILLIARD

DAN REZNIK*, RONALDO GARCIA, AND MARK HELMAN

ABSTRACT. Inverting the vertices of elliptic billiard N -periodics with respect to a circle centered on one focus yields a new “focus-inversive” family inscribed in Pascal’s Limaçon. The following are some of its surprising invariants: (i) perimeter, (ii) sum of cosines, and (iii) sum of distances from inversion center (the focus) to vertices. We prove these for the $N=3$ case, showing that this family (a) has a stationary Gergonne point, (b) is a 3-periodic family of a second, rigidly moving elliptic billiard, and (c) the loci of incenter, barycenter, circumcenter, orthocenter, nine-point center, and a great many other triangle centers are circles.

Keywords invariant, elliptic, billiard, inversion.

MSC 51M04 and 51N20 and 51N35 and 68T20

1. INTRODUCTION

In [17] we introduced the “focus-inversive” polygon, whose vertices are inversions of elliptic billiard N -periodic vertices with respect to a circle centered on one focus. Since N -periodics are inscribed in an ellipse, the focus-inversive family will be inscribed in Pascal’s Limaçon [4]; see Figure 1, and is therefore non-Ponceletian.

A classic invariant of billiard N -periodics is perimeter [22]. Recently, the sum of cosines was proved as an interesting dependent¹ invariant [1, 2]. Experimentally, for all N , the focus-inversive family conserves (i) the sum of distances from the focus to its vertices, (ii) perimeter, and (iii) the sum-of-cosines (except for $N = 4$). The first two have been recently proved [18].

In [20, Thm 1] the loci of classic centroids of Poncelet polygons are studied. It is shown that while vertex and area centroids always sweep out conics, the locus of the perimeter centroid is in general non-conic. Interestingly, for all N , we find that the loci of the 3 aforementioned centroids are *circles* over the focus-inversive family, though a proof is still pending.

Summary of the Article:

- **Section 2:** We review basic relations for the elliptic billiard.
- **Section 3:** The focus-inversive family derived from billiard 3-periodics is non-Ponceletian, and its caustic can be compact and regular but also contain cusps, and/or be non-compact. A special triangle center [23, Gergonne

D. Reznik*, Data Science Consulting, dreznik@gmail.com.

R. Garcia, Federal Univ. of Goiás, ragarcia@ufg.br.

M. Helman, Rice University, markhelman@hotmail.com.

¹Any “new” invariants are dependent upon the two integrals of motion – linear and angular momentum – that render the elliptic billiard an integrable dynamical system [9].

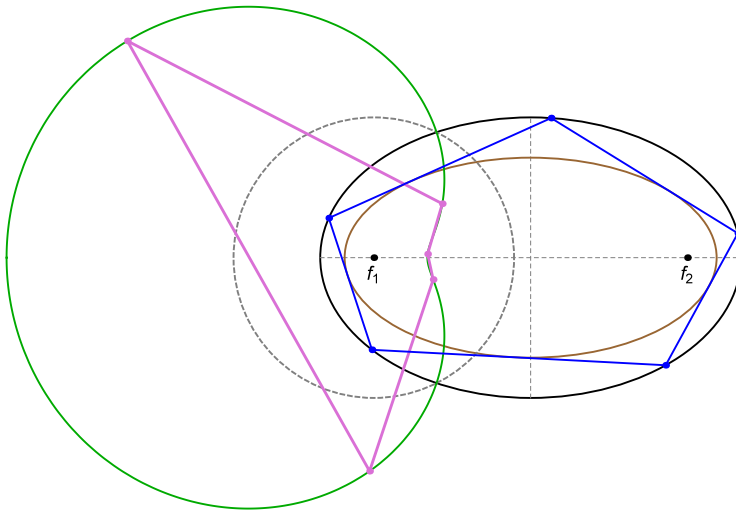


FIGURE 1. For a generic N -periodic (blue, $N=5$) with vertices P_i , the inversive polygon (pink) is inscribed in Pascal's Limaçon (green) and has vertices at inversions of the P_i with respect to a circle (dashed black) centered on f_1 . For all N , the focus-inversive perimeter, sum of cosines[‡], and sum of focus-to-vertex distances are experimentally invariant [17]; and a proof has recently appeared [18]. [‡] Sum of focus-inversive cosines is variable for $N=4$ simple and a certain self-intersected $N=6$ [6]. [Video](#).

Point] is stationary. Both perimeter and sum of cosines are invariant. Indeed, focus-inversive triangles are also billiard 3-periodics, but of a rigidly-moving billiard table, whose center moves along a circle. The sum of distances from the inversion center (a focus) to each vertex is invariant as is the product of areas of left- and right-focus-inversive triangles.

- [Section 4](#): the loci of 29 of the first 100 centers listed in [11] are *circles*, and these include the vertex, area, and perimeter centroids. “Why so many circles?” is an unanswered question. We derive expressions for some centers and radii of said loci. Indeed, based on experiments with 1000 triangle centers, we conjecture that if the locus of a triangle center in the billiard family is a conic, then it is a circle in the inversive family. Proofs are welcome.
- [Section 5](#): we study a closely-related, “center-inversive” family, whose vertices are inversions of billiard 3-periodics with respect to a circle concentric with the billiard. The family is also non-Ponceletian (inscribed in Booth's curve and circumscribing a non-conic caustic). We prove that the locus of the circumcenter is an ellipse; based on experiments, we conjecture said center to be the only one capable of producing a conic locus.

In [Appendix A](#) we review some classical quantities of the elliptic billiard. A reference table with all symbols used appears in [Appendix B](#). A link to a YouTube animation is provided in the caption of most figures. [Table 1](#) in [Section 6](#) compiles all videos mentioned.

Related Work. Experimentation with the dynamic geometry of 3-periodics in the elliptic billiard evinced that the loci of the incenter, barycenter, and circumcenter are ellipses. These observations were soon proved [5, 19, 20]. Indeed, using a combination of numerical and computer-algebra methods, we showed that the loci of a full 29 out of the first 100 centers listed in Kimberling’s Encyclopedia [11] are ellipses [7]. Odehnal’s studied the loci of triangle centers in the poristic family [12], detecting many as stationary (points), ellipses, and circles.

2. PRELIMINARIES

Throughout this article we assume the elliptic billiard is the ellipse:

$$f(x, y) = \left(\frac{x}{a}\right)^2 + \left(\frac{y}{b}\right)^2 = 1, \quad a > b > 0.$$

Let $\delta = \sqrt{a^4 - a^2b^2 - b^4}$ and ρ denote the radius of the inversion circle. The eccentricity $\varepsilon = \sqrt{1 - (b/a)^2}$, and $c^2 = a^2 - b^2$.

Recall the definition of a *triangle center*: these are points on the plane of a triangle defined by functions of their sidelengths and/or angles [10]. Centers will be referred to using the X_k notation, X_1 is the incenter, X_3 the circumcenter, in the manner of in Kimberling’s Encyclopedia [11]. Any symbols suffixed by \dagger (resp. \odot) refer to the focus-inversive (resp. center-inversive) triangle, e.g., X_9^\dagger is the mittenpunkt of the focus-inversive triangle, L^\dagger its perimeter, etc.

A word about our proof method. We omit most proofs as they have been produced by a consistent process, namely: (i) using an explicit expressions for billiard 3-periodic vertices (see [5, 15]), normally setting a first vertex $P_1 = (a, 0)$ so as to obtain an isosceles configuration; (ii) obtain a symbolic expression for the invariant of interest; (iii) simplify it (both human intervention and CAS); finally (iv) verify its validity symbolically and/or numerically over several N-periodic configurations and elliptic billiard aspect ratios a/b .

3. FOCUS-INVERSIVES AND THE ROTATING BILLIARD TABLE

A generic $N > 3$ focus-inversive polygon is illustrated in Figure 1. This is a polygon whose vertices are inversions of the N-periodic vertices wrt a circle of radius ρ centered on focus f_1 .

It is well known the inversion of an ellipse with respect to a focus-centered unit circle is a loopless Limaçon of Pascal $\mathcal{L}(t)$ [4], given by:

$$\mathcal{L}(t) = [-a \cos t(\varepsilon \cos t + 1) - c, a \sin t(\varepsilon \cos t + 1)], \quad 0 \leq t \leq 2\pi$$

Therefore:

Remark 1. For any N , the focus-inversive family is inscribed in $\mathcal{L}(t)$.

Figure 3 shows the non-conic “caustic” (envelope of sidelines) to the $N = 3$ focus-inversive family for various values of a/b . As a/b is increased, the caustic transitions from (i) a regular curve, to (ii) one with a self-intersection and two cusps, to (iii) a non-compact curve with two infinite branches.

Figure 2 illustrates the $N = 3$ focus-inversive triangle. Recall two well-known triangle centers: (i) the Gergonne point X_7 : this is where a triangle and its intouch (contact) triangle are perspective, see [23, Gergonne Point]; (ii) the Mittenpunkt

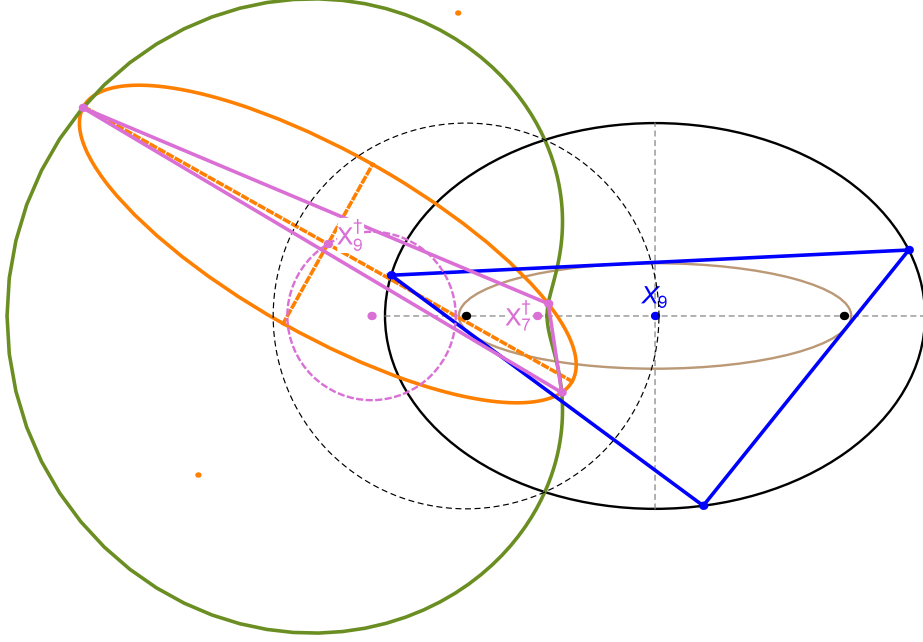


FIGURE 2. The vertices of 3-periodics (blue), when inverted with respect to a unit circle (dashed black) centered on a focus, produce a family of constant perimeter triangles (pink). Their X_9 -centered circumellipses (orange) rigidly translate and rotate (invariant semi-axes) with their center X_9^\dagger moving along a circle. The Gergonne point X_7^\dagger of the inversive family is stationary. [Video 1](#), [Video 2](#)

X_9 : where lines drawn from the excenters through the side midpoints concur [23, Mittenpunkt].

Proposition 1. *Over the 3-periodic family, the Gergonne point X_7^\dagger of focus-inversive triangles is stationary on the billiard's major axis at location:*

$$X_7^\dagger = \left[c \left(1 - \frac{\rho^2}{\delta + c^2} \right), 0 \right]$$

Note: let X_7^\ddagger denote the inversion of X_7^\dagger with respect to the same inversion circle used above. Then:

$$X_7^\ddagger = \left[\frac{\delta}{c}, 0 \right]$$

Proposition 2. *Over the 3-periodic family, the Mittenpunkt X_9^\dagger of focus-inversive triangles moves along a circle with center and radius given by:*

$$C_9^\dagger = \left[-c \left(1 + \rho^2 \frac{1}{2b^2} \right), 0 \right]$$

$$R_9^\dagger = \rho^2 \frac{2a^2 - b^2 - \delta}{2ab^2}$$

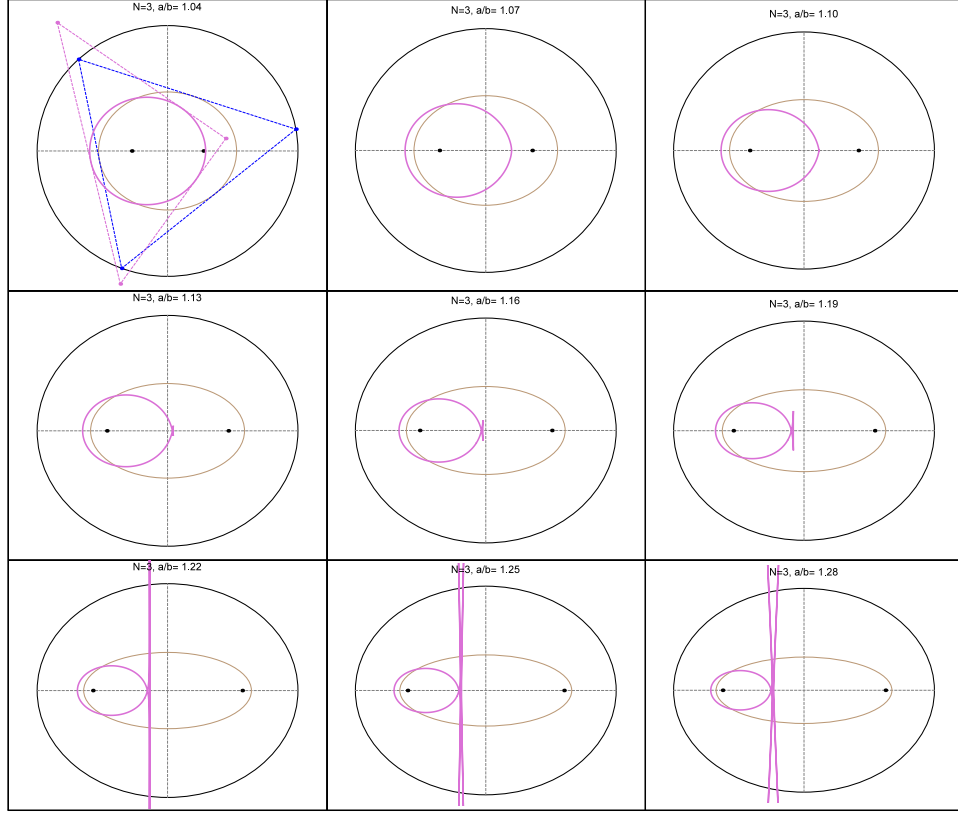


FIGURE 3. Non-conic caustic (pink) to the focus-inversive family (pink). As a/b increases, said caustic transitions from (i) regular, to (ii) a curve with one self-intersection and two cusps, to (iii) a non-compact curve. A sample 3-periodic (dashed blue) and the corresponding focus-inversive triangle (dashed pink) is shown on the first frame only. The billiard confocal caustic (brown) is shown on every frame. **App**

Remark 2. Let C_9^\dagger denote the inversion of C_9^\dagger with respect to the same inversion circle used above. Then:

$$C_9^\dagger = \left[-\frac{a^2 + b^2}{c}, 0 \right]$$

Proposition 3. The perimeter L^\dagger of the $N = 3$ focus-inversive family is invariant and given by:

$$L^\dagger = \rho^2 \frac{\sqrt{(8a^4 + 4a^2b^2 + 2b^4)\delta + 8a^6 + 3a^2b^4 + 2b^6}}{a^2b^2}$$

Surprisingly, perimeter invariance of the focus-inversive polygon has been generalized to all N [18].

Proposition 4. For $N = 3$, the sum of cosines of focus inversive triangles is given by:

$$\sum \cos \theta_{1,i}^\dagger = \frac{\delta(a^2 + c^2 - \delta)}{a^2c^2}$$

As seen above, the focus-inversive family simultaneously conserves perimeter and sum of cosines. Still referring to Figure 2:

Corollary 1. *With respect to a reference system centered on X_9^\dagger and oriented along the semi-axes of \mathcal{C}^\dagger , the inversive $N = 3$ family is a 3-periodic billiard family of \mathcal{C}^\dagger .*

Indeed, \mathcal{C}^\dagger can be regarded as the inversive triangle's rigidly-moving mittenpunkt-centered circumconic, called the “circumbilliard” in [14]:

Proposition 5. *The X_9^\dagger -centered circumellipse \mathcal{C}^\dagger of the $N = 3$ inversive family has invariant semi-axes a^\dagger and b^\dagger given by:*

$$\begin{aligned} a^\dagger &= \rho k_1 \sqrt{k_2 (\delta + a c)} \\ b^\dagger &= \rho k_1 \sqrt{k_2 (\delta - a c)} \end{aligned}$$

where:

$$\begin{aligned} k_1 &= \frac{c\sqrt{2}}{k_3} \sqrt{(8a^4 + 4a^2b^2 + 2b^4)\delta + 8a^6 + 3a^2b^4 + 2b^6} \\ k_2 &= 2a^2 - b^2 - \delta \\ k_3 &= 2ab^2 ((2a^2 - b^2)\delta + 2a^4 - 2a^2b^2 - b^4) \end{aligned}$$

More Focus-Inversive Invariants. As noted in Table 2, let $d_{1,i} = |P_i - f_1|$.

Proposition 6. *For $N = 3$, the sum of focus-inverse spoke lengths is invariant and given by:*

$$\sum \frac{1}{d_{1,i}} = \frac{a^2 + b^2 + \delta}{ab^2}$$

Referring to Figure 4:

Proposition 7. *For $N = 3$, the area product $A_1^\dagger A_2^\dagger$ of the two focus-inversive triangles is given by:*

$$A_1^\dagger A_2^\dagger = \frac{\rho^8}{8a^8b^2} \left[(a^4 + 2a^2b^2 + 4b^4)\delta + \frac{3a^4b^2}{2} + a^6 + 4b^6 \right]$$

Experiments suggest:

Conjecture 1. *Over billiard N -periodics, $N \geq 3$ is odd, the area product $A_1^\dagger A_2^\dagger$ is invariant.*

Observation 1. *The areas of both pedal triangles of the focus-inversives with respect to the respective foci are dynamically equal.*

4. CIRCULAR LOCI OF TRIANGLE CENTERS

In [7] we showed that amongst the first 100 triangle centers listed on [11], the following 29 sweep an elliptic locus over 3-periodics in the elliptic billiard: X_k , $k=1, 2, 3, 4, 5, 7, 8, 10, 11, 12, 20, 21, 35, 36, 40, 46, 55, 56, 57, 63, 65, 73, 78, 79, 80, 84, 88, 90, 100$. Notably, the Mittenpunkt X_9 is stationary at the billiard center [16].

Referring to Figure 5:

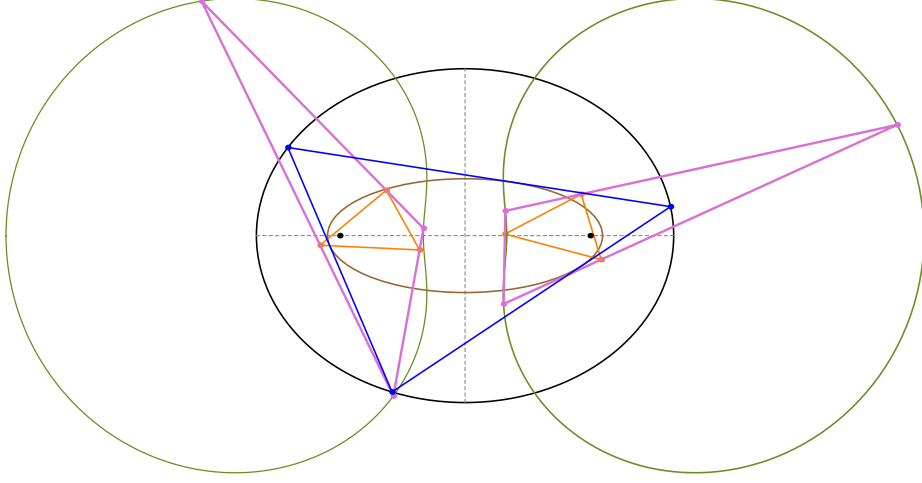


FIGURE 4. f_1 - and f_2 -inversive triangles are shown (pink). The product of their areas is invariant. Also shown are the f_1 - and f_2 -pedal polygons (orange) to said triangles. Their areas are variable but dynamically equal. [Video](#)

Theorem 1. *Amongst the first 100 triangle centers listed on [11], the following 28 sweep a circular locus over focus-inversive 3-periodics in the elliptic billiard: X_k^\dagger , $k=1, 2, 3, 4, 5, 8, 9, 10, 11, 12, 20, 21, 35, 36, 40, 46, 55, 56, 57, 63, 65, 73, 78, 79, 80, 84, 90, 100$. All centers lie on the billiard major axis.*

Proof. Symbolic manipulation and numeric verification. \square

Through painstaking CAS-assisted simplification, we were able to obtain compact expressions for only a few of the above circular loci, namely: $X_k, k=1, 2, 3, 4, 5, 9, 11, 100$.

Proposition 8. *The locus of X_1^\dagger is the circle given by:*

$$C_1^\dagger = \left[c \left(-1 + \rho^2 \frac{-2a^2 + b^2 + 2\delta}{2b^4} \right), 0 \right]$$

$$R_1^\dagger = \rho^2 \frac{-2\delta^2 + b^4 + (2a^2 - b^2)\delta}{2ab^4}$$

Proposition 9. *The locus of X_2^\dagger is the circle given by:*

$$C_2^\dagger = \left[-c \left(1 + \rho^2 \frac{2a^2 - b^2 - \delta}{3a^2b^2} \right), 0 \right]$$

$$R_2^\dagger = \rho^2 \frac{2a^2 - b^2 - \delta}{3ab^2}$$

Proposition 10. *The locus of X_3^\dagger is the circle given by:*

$$C_3^\dagger = \left[-c \left(1 + \rho^2 \frac{a^2 + b^2}{2b^4} \right), 0 \right]$$

$$R_3^\dagger = \rho^2 \frac{a(-b^2 + \delta)}{2b^4}$$

Proposition 11. *The locus of X_4^\dagger is the circle given by:*

$$C_4^\dagger = \left[c \left(-1 + \rho^2 \frac{(b^2 + \delta)\delta}{a^2 b^4} \right), 0 \right]$$

$$R_4^\dagger = \rho^2 \frac{c^2(b^2 + \delta)}{ab^4}$$

Proposition 12. *The locus of X_5^\dagger is the circle given by:*

$$C_5^\dagger = \left[c \left(-1 + \rho^2 \frac{a^4 - 3a^2 b^2 + 2b^4 + 2b^2 \delta}{4a^2 b^4} \right), 0 \right]$$

$$R_5^\dagger = \rho^2 \frac{(3a^2 - 2b^2)b^2 + (a^2 - 2b^2)\delta}{4ab^2}$$

Proposition 13. *The locus of X_{11}^\dagger is the circle given by:*

$$C_{11}^\dagger = \left[c \left(-1 + \rho^2 \frac{-a^2 + b^2 + \delta}{2a^2 b^2} \right), 0 \right]$$

$$R_{11}^\dagger = \rho^2 \frac{-a^2 + b^2 + \delta}{2ab^2}$$

Proposition 14. *The locus of X_{100}^\dagger is the circle given by:*

$$C_{100}^\dagger = \left[-c \left(1 + \rho^2 \frac{1}{b^2} \right), 0 \right]$$

$$R_{100}^\dagger = \rho^2 \frac{a}{b^2}$$

As noted above, the focus-inversive Gergonne point X_7^\dagger is stationary on the major axis.

In [15] triangle centers whose locus over 3-periodics was the billiard boundary were called “swans”. As it was shown, both X_{88} and X_{100} are swans [15]. Curiously, the former’s (resp. latter’s) motion is non-monotonic (monotonic) with respect to a continuous clockwise parametrization of 3-periodics.

Referring to Figure 7:

Observation 2. *Amongst all 29 triangle centers whose loci are ellipses over billiard 3-periodics, only X_{88}^\dagger does not sweep a circular locus over the focus-inversive family. Nevertheless, this locus is algebraic, regular, can be both convex and concave, and is symmetric wrt the major axis of the ellipse.*

Referring to Figure 6, X_{162} is yet another example of a billiard “swan” whose focus-inversive locus is non-elliptic.

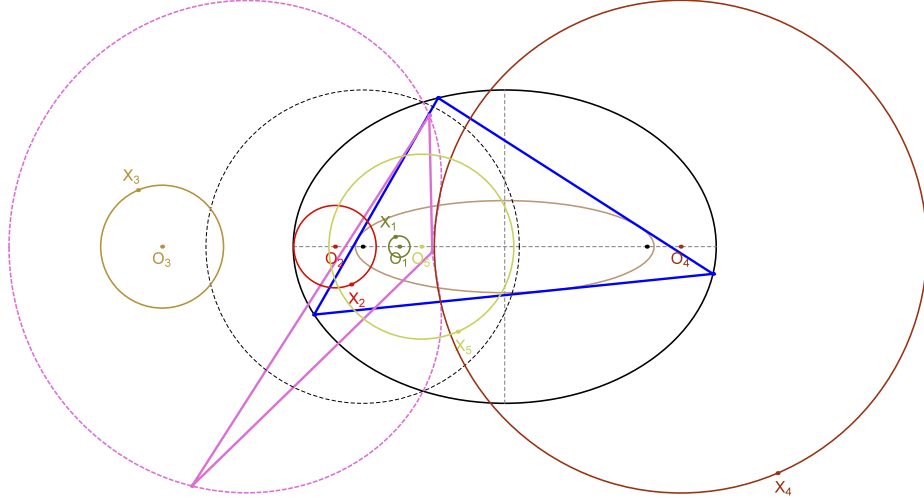


FIGURE 5. The focus-inversive 3-periodic (pink) is shown inscribed in Pascal's Limaçon (dashed pink). Also shown are the circular loci of X_k^\dagger , $k = 1, 2, 3, 4, 5$. Notice all its centers O_i lie on the billiard's major axis. [Video](#)

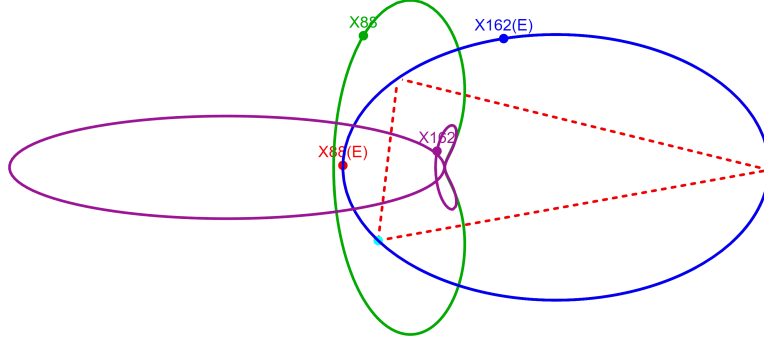


FIGURE 6. Over billiard 3-periodics (dashed red) the loci of both X_{88} and X_{162} coincide with the billiard (blue). However, when taken as centers of the the focus-inversive triangles (not shown), their loci are clearly non-elliptic (green and purple). Live app: [X88+X162](#), [X88+X100](#)

Observation 3. For $101 \leq k \leq 1000$, the following 68 focus-inversive triangle centers also sweep circular loci: X_k^\dagger , $k = 104, 119, 140, 142, 144, 145, 149, 150, 153, 165, 191, 200, 210, 214, 224, 226, 329, 354, 355, 376, 377, 381, 382, 388, 390, 392, 404, 405, 411, 442, 443, 452, 474, 480, 484, 495, 496, 497, 498, 499, 546, 547, 548, 549, 550, 551, 553, 631, 632, 908, 920, 934, 936, 938, 942, 943, 944, 946, 950, 954, 956, 958, 960, 962, 993, 997, 999, 1000$.

Referring to [Figure 7](#):

Observation 4. For $k \leq 1000$, the only triangle centers whose billiard locus is not an ellipse and whose focus-inversive locus is a circle are X_{150} and X_{934} . In fact, the latter's locus is identical to X_{100}^\dagger .

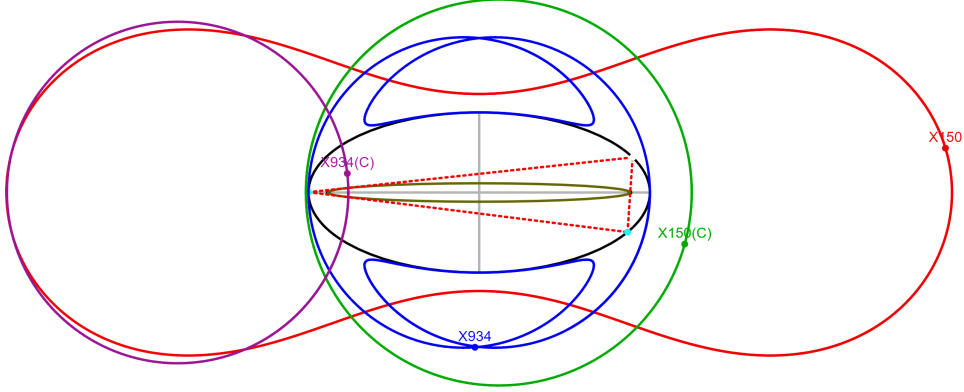


FIGURE 7. The locus of X_{150} is a dumbbell curve (red). Curiously, the locus of X_{150} over the focus inversives is a circle (green). Similarly, the billiard locus of X_{934} (blue) is a curve with two self-intersections; its locus over the focus-inversives is a circle.

App

Experimentally, in the range $k \leq 1000$, if the locus of X_k is an ellipse over billiard 3-periodics (excluding the cases where the locus is the billiard itself), then the locus of X_k^\dagger over the focus-inversive family is a circle. Therefore:

Conjecture 2. *If the the locus of some triangle center X is an ellipse over billiard 3-periodics, then the locus of X^\dagger over the inversive family is a circle.*

4.1. Locus of Perimeter Centroid. Let C_0, C_1, C_2 denote the vertex, perimeter, and area centroids of polygon, respectively. In [20, Thm 1] it was shown that the loci of C_0, C_2 over Poncelet families are ellipses, though this not hold in general for C_1 .

For triangles, $C_0 = C_2 = X_2$ and $C_1 = X_{10}$ [23, Spieker Center]. Per above we already know that the loci of X_2 and X_{10} over the focus-inversive family are circles. Therefore, and referring to Figure 8:

Corollary 2. *The loci of the $C_i^\dagger, i = 1, 2, 3$ of the focus-inversive family are circles.*

Surprisingly, experiments suggest:

Conjecture 3. *Over the focus-inversive family derived from billiard N -periodics, $N \geq 3$, the locus of vertex, perimeter, and area centroids are all circles.*

5. THE CENTER-INVERSIVE FAMILY

Let the *center-inversive triangle* have vertices at the inversions of the P_i w.r.t. unit-radius circle concentric with the elliptic billiard; see Figure 9. Therefore this family is inscribed in Booth's curve (the inverse of an ellipse with respect to a concentric circle) [3]. As shown in Figure 10, as a/b increases, the caustic transitions from a convex-regular curve, to one with two self-intersections and cusps, to a non-compact one.

Proposition 15. *The locus of the circumcenter X_3^\odot of the center-inversive triangle is an ellipse concentric, axis-aligned, and homothetic to the elliptic locus of X_3 of the billiard 3-periodics, at ratio $1/\delta$. Moreover, the aspect ratio of the locus of X_3^\odot is the reciprocal of that of the caustic.*

Proof. The circumcircle of the center-inversive triangle is the inversion of the circumcircle of the billiard's 3-periodic. Denote by R and X_3 the circumradius and circumcenter of the 3-periodic, and by X_3^\odot the circumcenter of the center-inversive triangle. By properties of circle inversion, we have that the center of the billiard O , X_3 , and X_3^\odot are collinear, with $OX_3^\odot = \frac{OX_3}{OX_3^2 - R^2}$ (recall that the inversion of the center of a circle does not coincide with the center of the inverted circle). The quantity $OX_3^2 - R^2$ represents the power of point O with respect to the circumcircle of the 3-periodic. In [8, Thm 3], it was shown that the power of the billiard center with respect to this circumcircle is constant over the family of 3-periodics and equal to $-\delta$. Moreover, in [5] it was proved that the locus of X_3 is an ellipse axis-aligned and concentric with the billiard and similar to the caustic (rotated by $\pi/2$). Thus, the locus of X_3^\odot must be an ellipse concentric, axis-aligned, and homothetic to that one at a ratio of $1/\delta$. \square

Conjecture 4. *The circumcenter X_3 is the only triangle center whose locus over the center-inversive family is a conic.*

Animations illustrating some focus-inversive phenomena are listed on [Table 1](#).

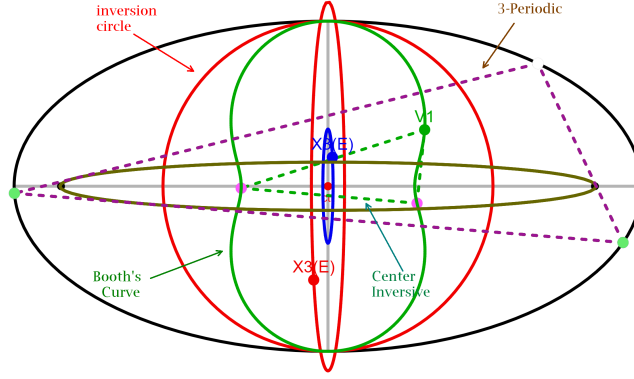


FIGURE 9. The center-inversive triangle (green) has vertices at the inversions of the 3-periodic vertices wrt unit-circle (red) concentric with the ellipse. It is inscribed in Booth's curve (green) [3]. Over the 3-periodics, the locus of X_3 is an ellipse (red) [5]. The locus of X_3 of the center-inversives is also an ellipse (blue), concentric, axis-aligned, and homothetic to the former at ratio $1/\delta$. App

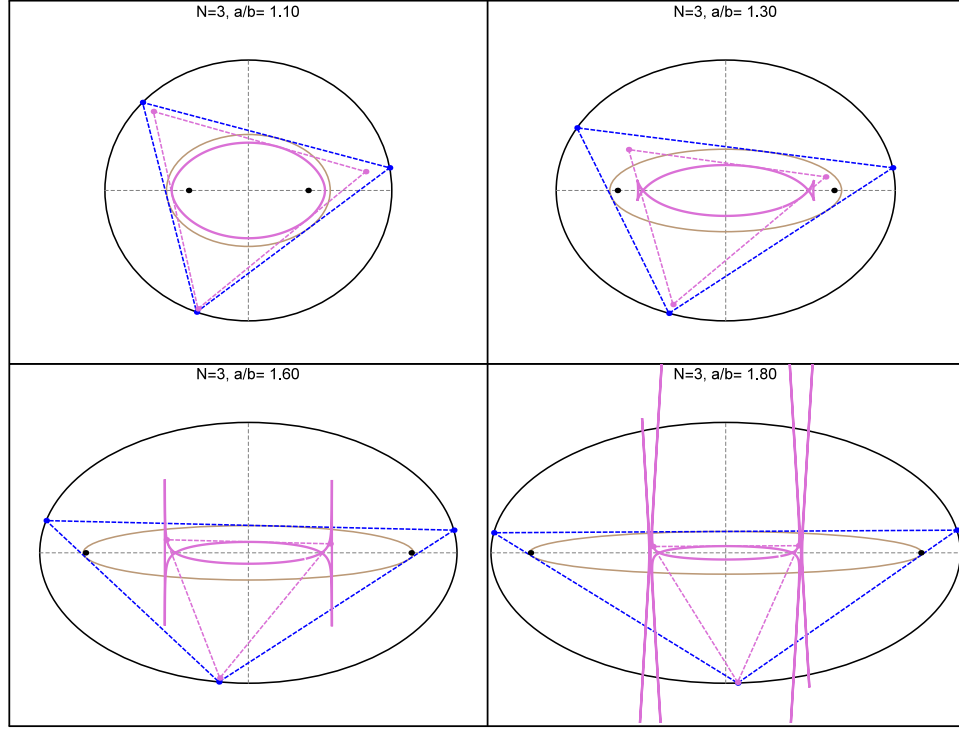


FIGURE 10. Non-conic caustic (pink) to the center-inversive family (dashed pink). As a/b increases it transitions from (i) a regular-convex curve, to (ii) one with two self-intersections and four cusps, to (iii) a non-compact, self-intersected curve. App1, App2

id	Title	youtu.be/<...>
01	N=5 invariants	wkstGKq5j0o
02a	N=3 circumbilliard I	LOJK5izTctI
02b	N=3 circumbilliard II	Y-j5eXqKGQE
03	N=3 invariant area product	OL2uMk2xyKk
04	N=5 invariant area product	bTkbdEPNUOY
05	N=3 equal-area pedals	OL2uMk2xyKk
06a	N=3 circular loci I	OAD2hpCRgCI
06b	N=3 circular loci II	tKB-50zW8F4
06c	N=3 circular loci III	srjm23nQbMc

TABLE 1. Videos of some focus-inversive phenomena. The last column is clickable and provides the YouTube code.

ACKNOWLEDGMENTS

We would like to thank Arseniy Akopyan, Peter Moses, and Pedro Roitman for useful insights.

The second author is fellow of CNPq and coordinator of Project PRONEX/CNPq/ FAPEG 2017 10 26 7000 508.

APPENDIX A. REVIEW: ELLIPTIC BILLIARD

Joachimsthal's Integral expresses that every trajectory segment is tangent to a confocal caustic [22]. Equivalently, a positive quantity J remains invariant at every bounce point $P_i = (x_i, y_i)$:

$$J = \frac{1}{2} \nabla f_i \cdot \hat{v} = \frac{1}{2} |\nabla f_i| \cos \alpha$$

where \hat{v} is the unit incoming (or outgoing) velocity vector, and:

$$\nabla f_i = 2 \left(\frac{x_i}{a^2}, \frac{y_i}{b^2} \right).$$

Hellmuth Stachel contributed [21] an elegant expression for Joachimsthal's constant J in terms of EB semiaxes a, b and the major semiaxes a'' of the caustic:

$$J = \frac{\sqrt{a^2 - a'^2}}{ab}$$

The signed area of a polygon is given by the following sum of cross-products [13]:

$$A = \frac{1}{2} \sum_{i=1}^N (P_{i+1} - P_i) \times (P_i - P_{i+1})$$

Let $d_{j,i}$ be the distance $|P_i - f_j|$. The inversion $P_{j,i}^\dagger$ of vertex P_i with respect to a circle of radius ρ centered on f_j is given by:

$$P_{j,i}^\dagger = f_j + \left(\frac{\rho}{d_{j,i}} \right)^2 (P_i - f_j)$$

N=3 case. For $N = 3$ the following explicit expressions for J and L have been derived [8]:

$$J = \frac{\sqrt{2\delta - a^2 - b^2}}{c^2}$$

$$L = 2(\delta + a^2 + b^2)J$$

When $a = b$, $J = \sqrt{3}/2$ and when $a/b \rightarrow \infty$, $J \rightarrow 0$.

APPENDIX B. TABLE OF SYMBOLS

symbol	meaning
O, N	center of billiard and vertex count
L, J	perimeter and Joachimsthal's constant
a, b	billiard major, minor semi-axes
a'', b''	caustic major, minor semi-axes
f_1, f_2	foci
P_i, θ_i	N -periodic vertices and angle
$d_{j,i}$	distance $ P_i - f_j $
A	N -periodic area
ρ	radius of the inversion circle
$P_{j,i}^\dagger$	vertices of the inversive polygon wrt f_j
L_j^\dagger, A_j^\dagger	perimeter, area of inversive polygon wrt f_j
$\theta_{j,i}^\dagger$	i th angle of inversive polygon wrt f_j

TABLE 2. Symbols used in the invariants. Note $i \in [1, N]$ and $j = 1, 2$.

REFERENCES

- [1] Akopyan, A. (2012). Conjugation of lines with respect to a triangle. *Journal of Classical Geometry*, 1: 23–31. [1](#)
- [2] Bialy, M., Tabachnikov, S. (2020). Dan Reznik's identities and more. *Eur. J. Math.* doi:10.1007/s40879-020-00428-7. [1](#)
- [3] Ferréol, R. (2020). Booth's curve. Mathcurve Portal. <https://mathcurve.com/courbes2d.gb/booth/booth.shtml>. [10](#), [12](#)
- [4] Ferréol, R. (2020). Pascal's limaçon. Mathcurve Portal. <https://mathcurve.com/courbes2d.gb/limaçon/limaçon.shtml>. [1](#), [3](#)
- [5] Garcia, R. (2019). Elliptic billiards and ellipses associated to the 3-periodic orbits. *American Mathematical Monthly*, 126(06): 491–504. [3](#), [11](#), [12](#)
- [6] Garcia, R., Reznik, D. (2020). Invariants of self-intersected and inversive N -periodics in the elliptic billiard. arXiv:2011.06640. [2](#)
- [7] Garcia, R., Reznik, D., Koiller, J. (2020). Loci of 3-periodics in an elliptic billiard: why so many ellipses? arXiv:2001.08041. [3](#), [6](#)
- [8] Garcia, R., Reznik, D., Koiller, J. (2020). New properties of triangular orbits in elliptic billiards. *Amer. Math. Monthly*, to appear. [11](#), [14](#)
- [9] Kaloshin, V., Sorrentino, A. (2018). On the integrability of Birkhoff billiards. *Phil. Trans. R. Soc.*, A(376). [1](#)
- [10] Kimberling, C. (1993). Triangle centers as functions. *Rocky Mountain J. Math.*, 23(4): 1269–1286. doi.org/10.1216/rmjm/1181072493. [3](#)

- [11] Kimberling, C. (2019). Encyclopedia of triangle centers. faculty.evansville.edu/ck6/encyclopedia/ETC.html. 2, 3, 6, 7
- [12] Odehnal, B. (2011). Poristic loci of triangle centers. *J. Geom. Graph.*, 15(1): 45–67. 3
- [13] Preparata, F., Shamos, M. (1988). *Computational Geometry - An Introduction*. Berlin: Springer-Verlag, 2nd ed. 13
- [14] Reznik, D., Garcia, R. (2021). Circuminvariants of 3-periodics in the elliptic billiard. *Intl. J. Geometry*, 10(1): 31–57. 6
- [15] Reznik, D., Garcia, R., Koiller, J. (2020). The ballet of triangle centers on the elliptic billiard. *Journal for Geometry and Graphics*, 24(1): 79–101. 3, 8
- [16] Reznik, D., Garcia, R., Koiller, J. (2020). Can the elliptic billiard still surprise us? *Math Intelligencer*, 42: 6–17. 6
- [17] Reznik, D., Garcia, R., Koiller, J. (2021). Fifty new invariants of N-periodics in the elliptic billiard. *Arnold Math. J.* doi:10.1007/s40598-021-00174-y. 1, 2
- [18] Roitman, P., Garcia, R., Reznik, D. (2021). New invariants of Poncelet-Jacobi bicentric polygons. arXiv:2103.11260. 1, 2, 5
- [19] Romaskevich, O. (2014). On the incenters of triangular orbits on elliptic billiards. *Enseign. Math.*, 60(3-4): 247–255. 3
- [20] Schwartz, R., Tabachnikov, S. (2016). Centers of mass of Poncelet polygons, 200 years after. *Math. Intelligencer*, 38(2): 29–34. 1, 3, 10
- [21] Stachel, H. (2020). Expression for Joachimsthal’s constant. Private Communication. 13
- [22] Tabachnikov, S. (2005). *Geometry and Billiards*, vol. 30 of *Student Mathematical Library*. Providence, RI: American Mathematical Society. bit.ly/2RV04CK. 1, 13
- [23] Weisstein, E. (2019). Mathworld. mathworld.wolfram.com. 2, 3, 4, 10